Particle Image Velocimetry and Numeric Analysis of Sand Deformations under a Test Plate

G. G. Boldyrev
Penza State University of Architecture and Construction, Penza, Russia

A.V. Melnikov
Penza State University of Architecture and Construction, Penza, Russia

V.A. Barvashov
R&D Center "Construction", Gersevanov Research Institute of Foundations, Moscow, Russia

ABSTRACT: The paper presents experimental and theoretical results of models tests of sand deformations under a test plate in plain strain. Sand base with and without reinforcement was tested. Strip footing model was loaded stepwise to ultimate loads. Vertical and lateral displacements dependence on reinforcement rate was compared with numerical results. Analysis of the obtained data yielded quantitative and qualitative conclusions.

1 INTRODUCTION

One of the methods used for strain behavior investigation is the photo-fixation of particle displacements, invented by a Russian engineer V.I. Kurdumov in 1889 and implemented by M.V. Malychev (1953). Sand particle displacement paths under a test plate are shown on Fig.1.

This method was further developed by Roscoe et al., (1963), who applied X-rays to measure soil strains by lead shots markers monitoring.

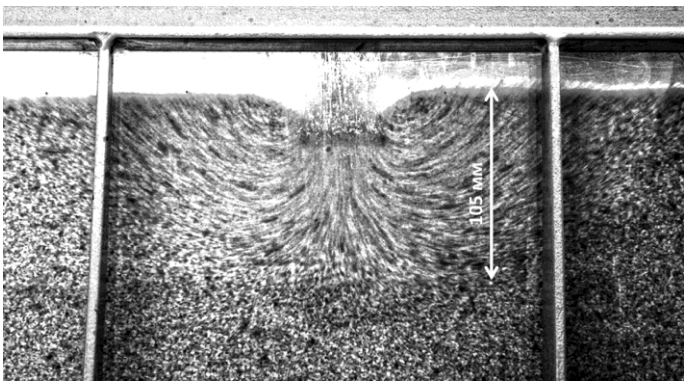

Fig.1 Particle displacement paths

Boldyrev and Nikitin (1986) applied photogrammetry technique to measure strains in sand bases. Two photos were compared prior and after the test to assess displacements of markers, placed at nodes of a grid. A pair of photographs was used to measure sand displacements versus *X* and Y axes prior and after the tests with the help of Geneva – Meter (accuracy class 0.2mm). The shear strain isolines are shown on Fig.2, showing that strains develop progressively from the plate edge to the free surface, enveloping a non-deformed zone (1) with neither shear nor volume strains.

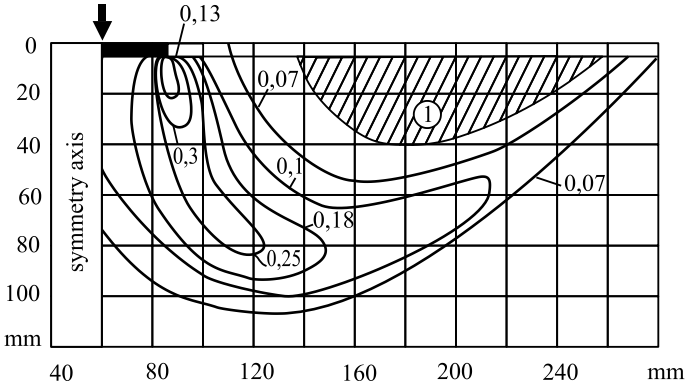

Рис. 2. Shear strain isolines: 1 – non-deformed zone; 2 –shear strain zone (Boldyrev and Nikitin, 1986). Не указана зона 2

In 2011 White proposed a velocity measuring technique for soil strains r in model plate tests. As compared to the X-ray the PIV technique is less time consuming and is currently used for model tests.

Particle Image Velocimetry (PIV) –is a technique used for processing digital images for determination of displacement fields. PIV was originally developed by Adrian (1991) for speed measuring in the field of fluid and gas mechanics. White (2001) was first to apply a modified approach while geotechnical tests.

PIV is applied to image strained surfaces by means of a photo-camera i.e. to investigationof reinforced bases in plain strain conditions using boxes with different test plates (Bostwick et al, 2010), pile models (Ni et al., 2010), triaxial compression tests (Sevi et al.2009; Datton et al, 2011).

2 MEASUREMENT TECHNIQUE

The purpose of this research was to investigate plain strain behavior of sand with and without reinforcement, loaded with a test plate.

Two groups of tests were done. In the first group the non-reinforced sand base deformations were registered. In the second group of tests a reinforcing 8x8 mm 1.5 mm thick geo-grid was placed at different depths (Fig.3).

The test load on the geo-grid sample showed that 12kN/m load produced 2% strain while tensile strength was 50kN/m.

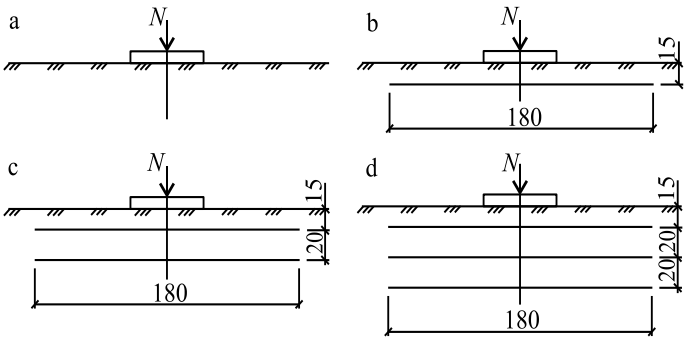

Fig. 3.Different sand reinforcements a – non-reinforced; b – one reinforcement layer; c – two-layer reinforcement; d – three-layer reinforcement.

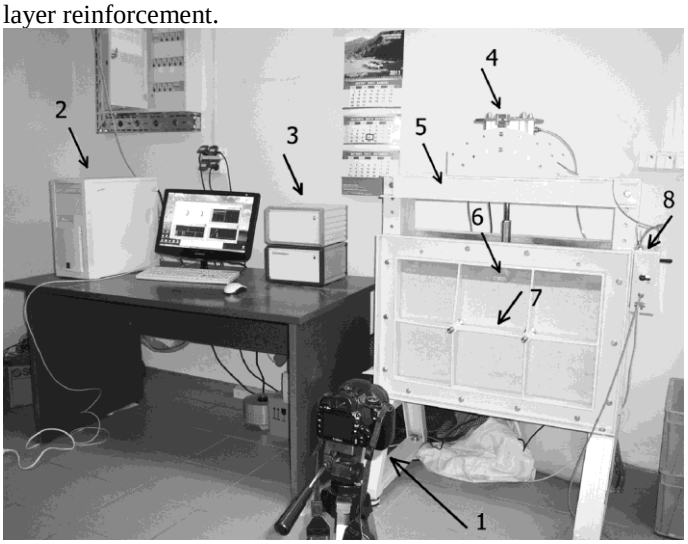

Рис. 4. Automated foundation model test set-up: 1 – Photocamera; 2 –PC; 3 – signal transmission unit; 4 – pneumatic loading unit; 5 –support beam; 6 –load test plate with a rod; 7 – plexiglass wall with stiffener; 8 – pressure control unit

The tests were conducted, using an automated facility (Fig.4), consisting of a 720x480x155mm box with translucent plexiglass. The walls were strengthened with steel stiffeners to bear lateral soil pressure.

The load was applied to a 50 mm large and 155 mm long test plate by means of pneumatic loading unit. For conducting automated loading procedure and for drawing graphs Geoteck-Foundation Software (www.npp-geotek.ru) was used for automatic loading, and the images were made digital camera Canon EOS 400D providing 10MP sensor with 3888x2592 resolution.The camera was placed at 2.5m from the box perpendicular to its translucent wall, it was connected to PC via USB.

Photos were taken automatically at each loading stage in order to avoid displacement of the camera.

Box plane was located precisely parallel to the CCD plane (camera matrix), however, the short focus lense made the image spherical. Therefore, 1 mm dia reference markers were fixed on the interior surface of the transparent plexiglass wall for the image sphericity correction.

Zhao and Ge (2008) proposed more difficult procedures of calibration using neural networks of the type back propagation perception.

Clean quartz sand was used. Its grain size distribution is given in Table 1.

Table 1. Sand grain size

Particle size, mm	<0,25	0,25-0,5	0,5-1	1-2	2-3
particle content by weight, %	0,1	0,2	1,9	60,9	36,9

Triaxial test data and “shear strain – stress deviator” curves (Fig.5) yielded shear stress limit equal to 0, 04. Table 5 shows that the shear stress limit dependence on confined pressure.

Sand was placed in the box by 10 mm layers and compacted with a flat plate to density $\rho = 1{,}59$ g/cm^3, porosity e =0,502, and shear resistance angle $\varphi = 37^o$. The average density was determined as the ratio of total mass over volume of the whole box.

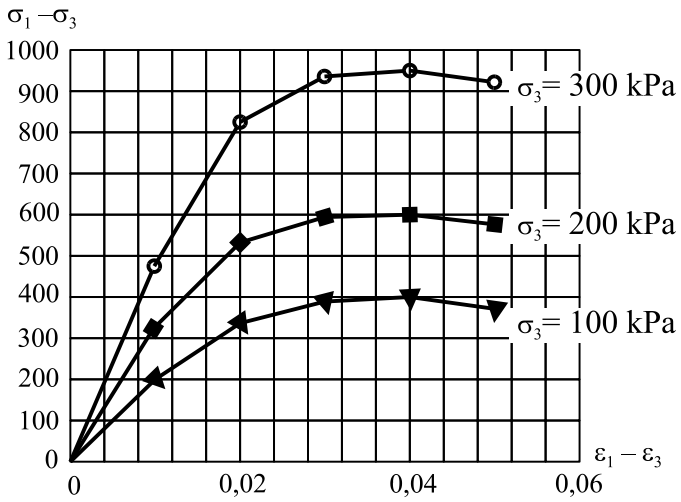

Fig.5. Shear strain – stress deviator plot

The load was applied to the test plate by stages with 15 min stabilization time at each stage.

3 UNREINFORCED SAND TEST DATA

Fig. 6 shows test plate stamp settlement versus pressure dependence. The loading stages are numbered. 0-1 segment (Fig. 7) shows sand deformations in

stage (0-1). Soil deformations show linearity versus test load. At stage (1-2) inelastic shear deformations appear, i.e. the stress- deformation curve is nonlinear. Stiff soil core forms under the plate and forces sand sideways that results in increased settlement. At the last stage (2-3) continuous shear surfaces form up resulting in instability.

The following data was obtained by software processing (http://www.pivtec.com): particle displacement vectors, particle vertical and lateral displacements, shear and volume strain. Shear strain was defined as $\gamma = \varepsilon_x - \varepsilon$ and volume strain as: $\gamma = \varepsilon_x + \varepsilon_y$.

The test accuracy was 0.1mm, which is certainly worse than that of PIV. This resulted from: sand against glass, unsteady camera focusing, camera vibrations, light intensity variations, local displacement rate, inaccuracy of markers positioning, pixel data conversion precision.

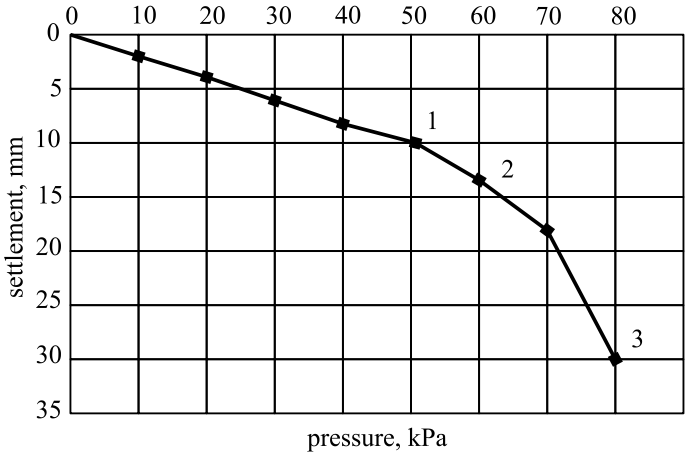

Fig.6. Settlement-load curve

Figs. 7-11 show graphical images of the test data.

Fig.7 shows two zones: 1 – compaction (-), patch 2 – uplift (+). The zones change with the external load growth.

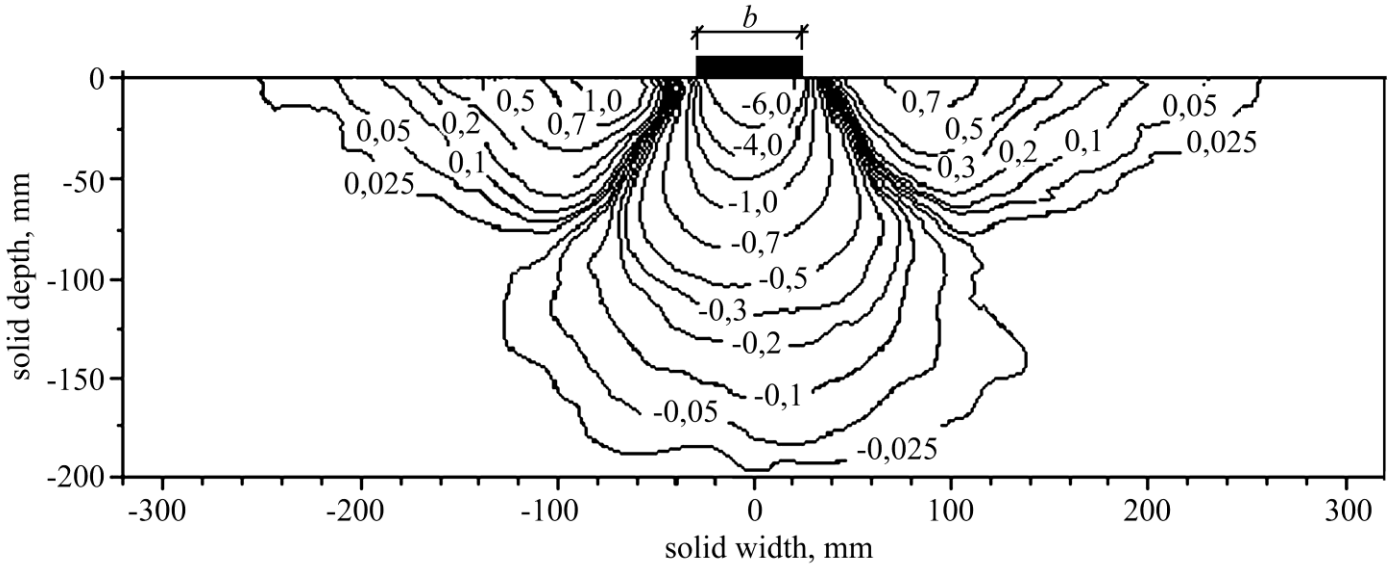

Fig.7. Vertical displacement isolines at 8 mm plate settlement: 1 – compaction – 1; 2 – uplift.

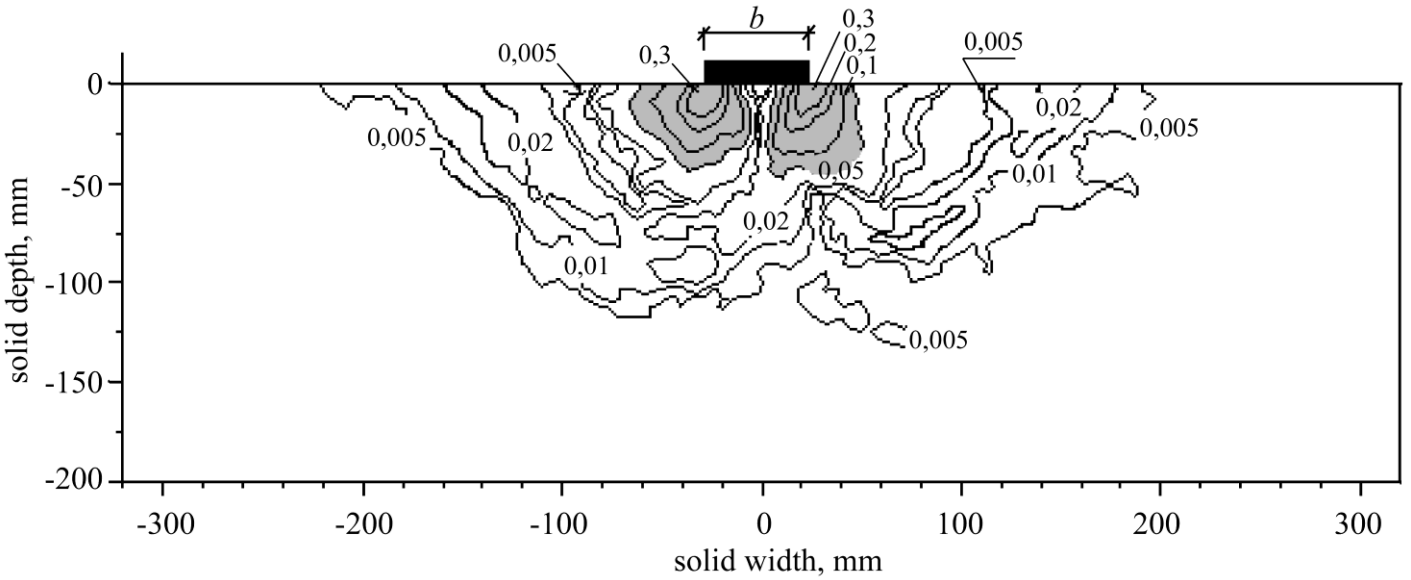

Fig.8. Shear strain isolines at 8 mm plate settlement

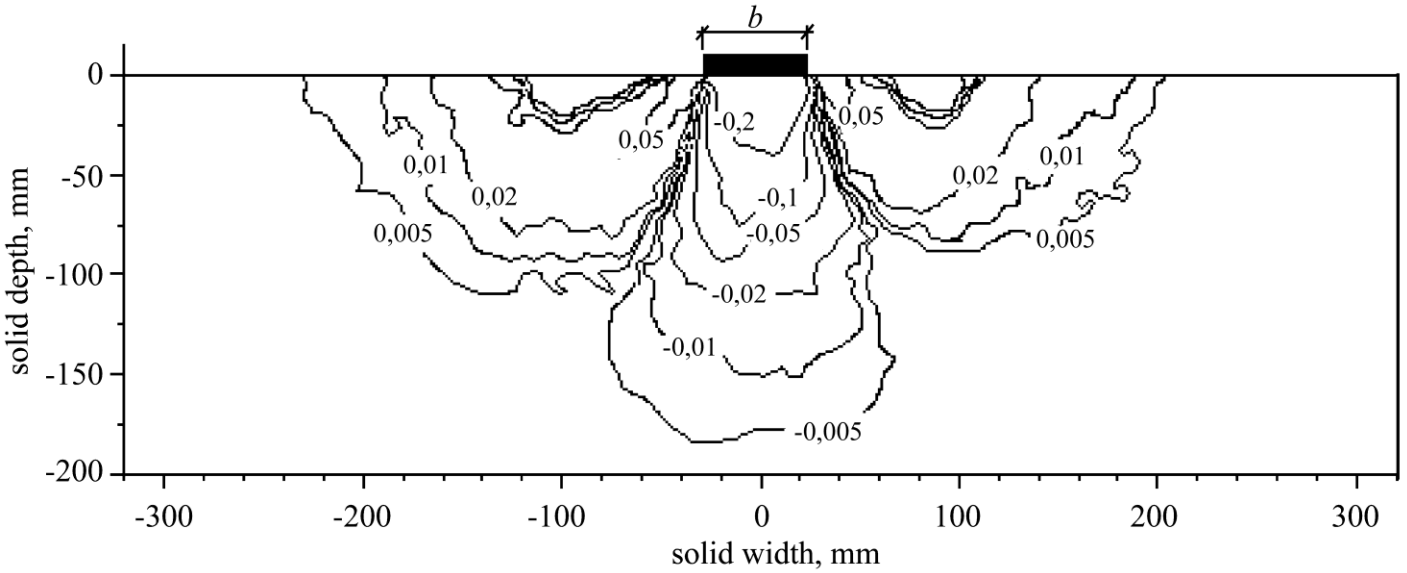

Fig.9. Volume strain isolines at 8 mm settlement

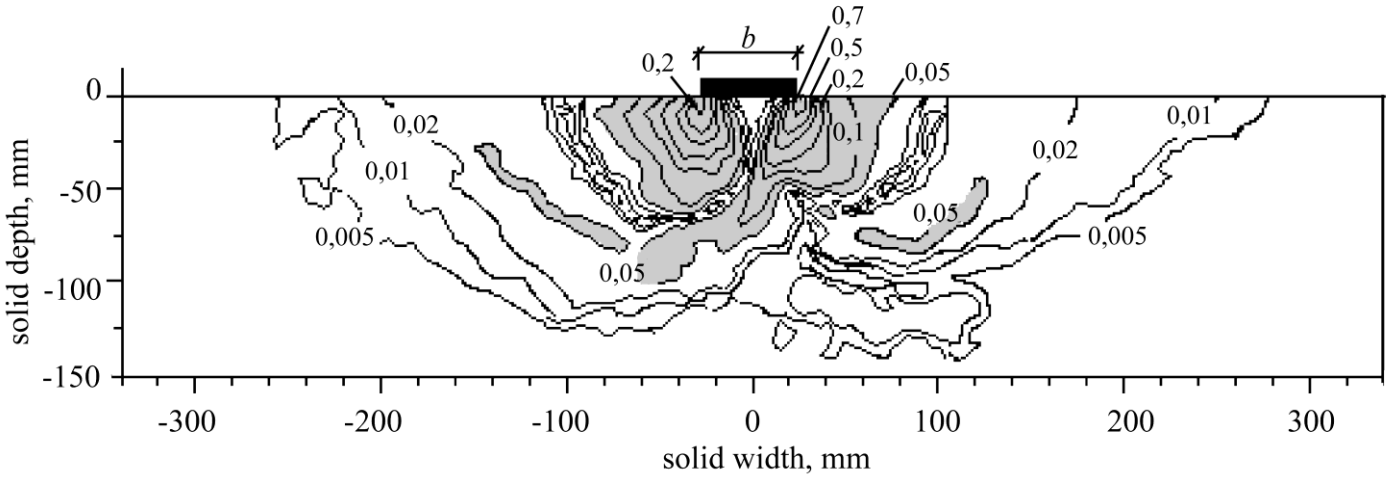

Fig.10. Shear strain isolines at 16 mm settlement

At the end of linear settlement-pressure curve (fig.6, zone 0-1) ultimate strains γ_{ult} = 0. 04 (fig. 4) develop at the depth equal to the plate width, *b* (Fig. 7). 16 mm zone corresponds to the change from nonlinear to intensive plastic strains and the growth of the plastic strain zone depth to 2*b* (Fig. 9). At the plate edges the strains PIV technique registers ultimate strain excess up to 7.5-fold and 17.5-fold respectively (Fig. 8,10). When the load is close to the ultimate value the shear strain develops both in the plate adjacent zone and on the free surface. (II, Fig.10). The then maximum shear concentrate in.

Due to sand compaction the measured test plate settlements are equal to those of the sand just in a small zone right under the plate bottom. The compacted sand wedge forms up under the plate as is shown by vertical displacement isolines due to sand compaction (Fig. 9). Then a compacted zone deepens asymmetrically to the plate (Fig. 7). Fig.8 shows two zones under the plate, having different volume strains: compaction (positive) and dilatancy (negative). Then the zone reaches the plate bottom. As is mentioned above, below the plate edges maximum shear strains develop downward and inside the plate (Fig. 8, 10) thus results in reducing the plastic zone and forming a wedge.

As is known [11] soil base instability results from shear zone formation under plate edges and its downward growth.

4 REINFORCED SAND TESTS

Fig.11 shows test plate settlement versus pressure plots for different reinforcement rates, points on the plots show, where PIV processing was done. Fig.11 shows that reinforcement changes pressure-settlement behavior. Settlements decrease if sand base stiffness growth.

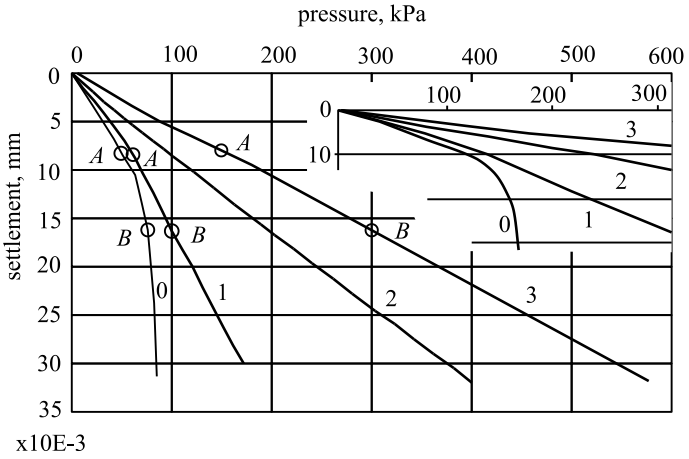

Fig. 11.Plate settlement versus loads plots: 1 – no reinforcement; 2,3,4 – 1,2,3 layers of reinforcement; A and B –PIV measurement points.

Ultimate load is greater for higher reinforcement rates, and the pressure-settlement curve becomes almost linear.

Figs.12-15 show reinforced sand shear and volume strain isoline. The reinforcement does not reduce shear strains under the plate edges.

Figs. 8, 12, 13 show that the maximum shear strain in sand above one layer of reinforcement is equal to 0.3, it is equal to 0.2 for one to three layers of reinforcement. It is evidently due the reinforcement being too low: 0.3b (15 mm), and does not prevent the shear strain progress this sand layer.

The reinforcement effect is much more pronounced close to ultimate load. Shear zones (Figs. 14, 15) develop downward and away from the plate axis. The location of strip-shaped shear is less.

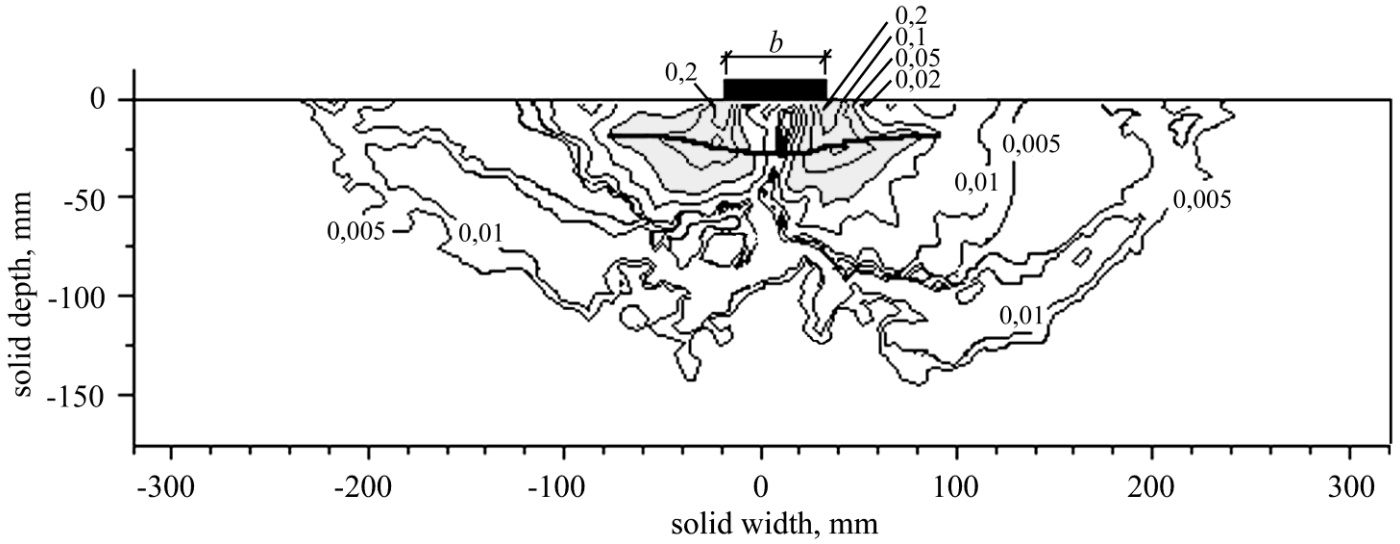

Fig. 12. 8mm plate loading. Shear strain isolines for one layer of reinforcement,

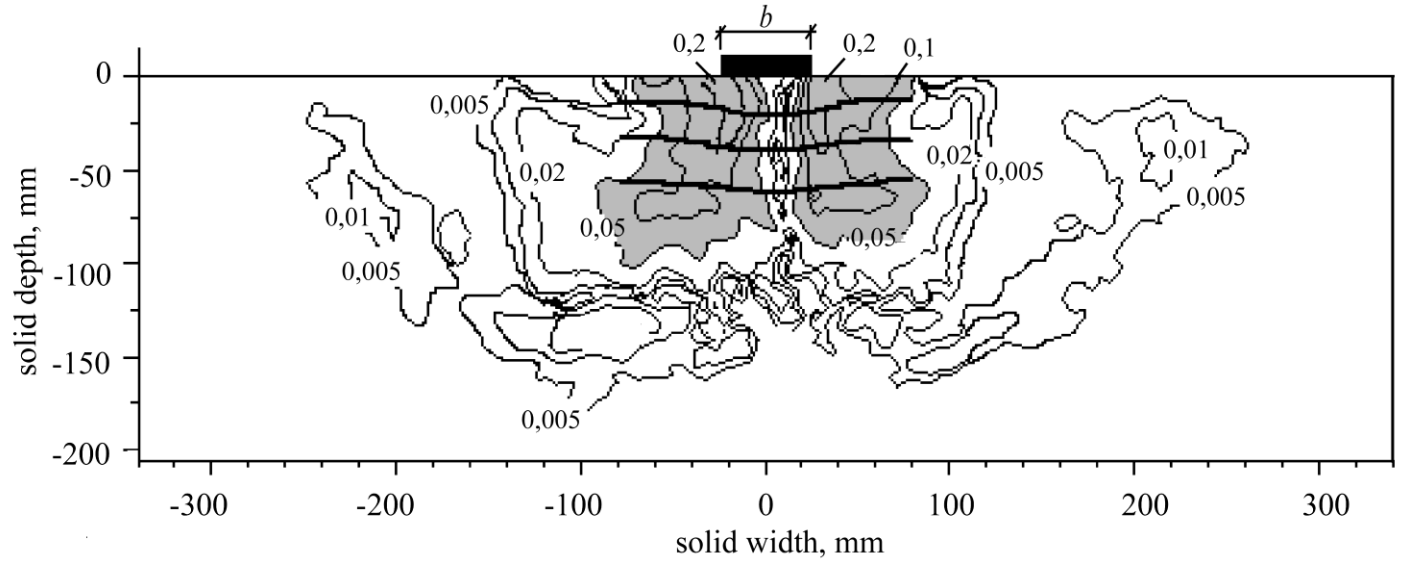

Fig. 13. 8 mm plate loading. Shear strain isolines for three grid layer reinforcement8mm stamp settlement

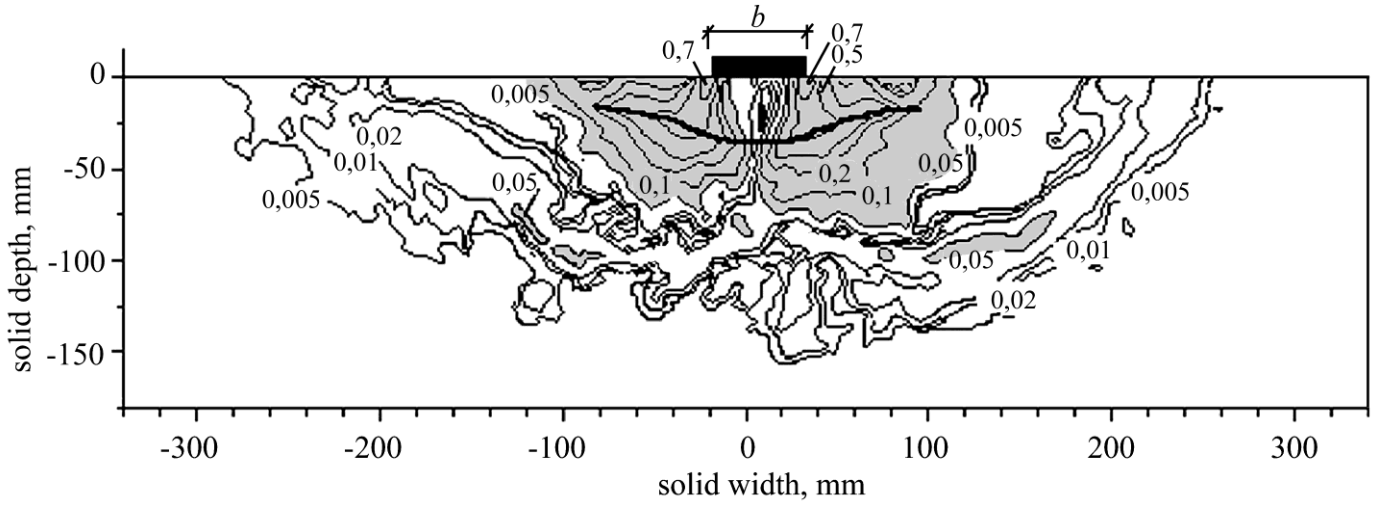

Fig. 14. 16 mm plate loading. Shear strain isolines for one layer of reinforcement.

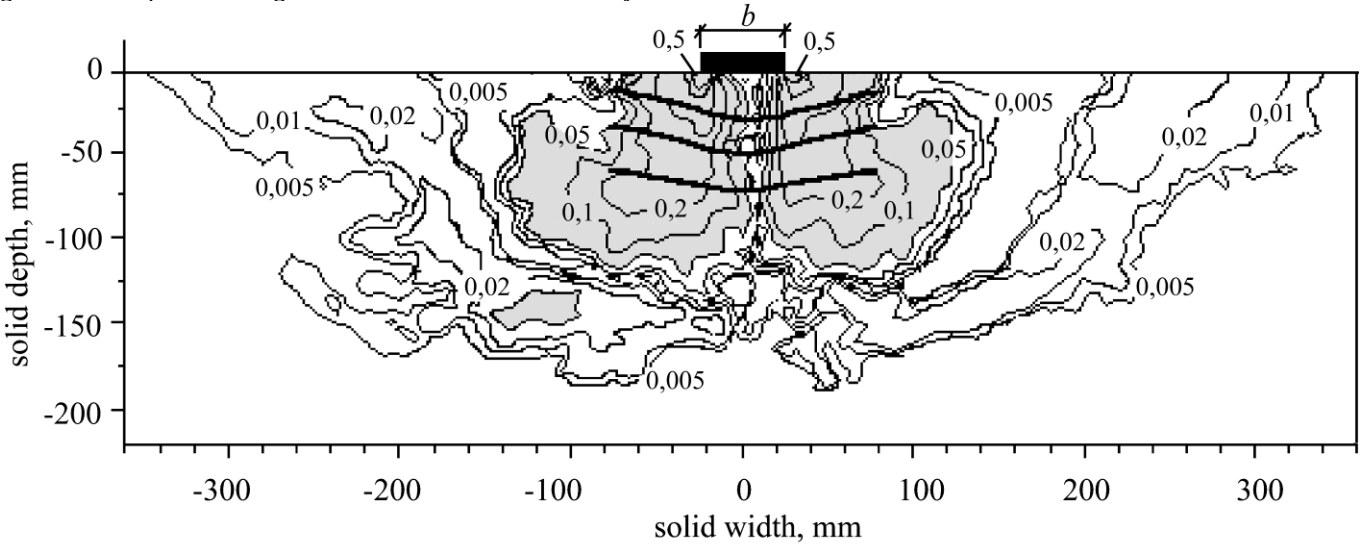

Fig. 15. !6 mm plate loading. Shear strain isolines for three-layer reinforcement

5 CONCLUSIONS

1. PIV technique is as effective for imaging strains in sand as photogrammetry.
2. PIV is more effective than photo-fixation technique in that it enables registration of both qualitative and qualitative features of sand strain behavior.
3. Shear strains under test plate edges are times 7 to 17 greater that those corresponding to the external load growth.
4. Shear strains develop deep down with the growth of external load.
5. Shear strains in sand with no reinforcement tend to localize in narrow strips.
6. Sand reinforcement increases the ultimate load on test plate, reduces plate settlements and expansion of the shear strain zone.

6 REFERENCES

Болдырев, Г.Г. и Никитин, Е.В. 1986. Деформация песка в основании плоского штампа. *Основания, фундаменты и механика грунтов*. №1: 26-28.

Курдюмов, В.И. 1891. К вопросу о сопротивлении оснований. Фотографический способ исследования процесса разрушения песчаного слоя под влиянием местной нагрузки. Вторая публичная лекция 11 декабря 1889 г. Санкт-Петербург.

Малышев, М.В. 1953.Теоретические и экспериментальные исследования несущей способности песчаного основания. *Лаборатория оснований и фундаментов. Информационные материалы. №2*. Москва: Водгео..

Цытович Н.А. 1983. Механика грунтов (краткий курс). Москва.

Adrian, R. J. 1991. Particle-Imaging Techniques for Experimental Fluid Mechanics. *Annual Review of Fluid Mechanics*. Vol. 23: 261-304.

Bostwick, L., Rowe, R. K., Take, W. A., Brachman, R. W. I. 2010. Anisotropy and directional shrinkage of geosynthetic clay liners. *Geosynthetics International*. No. 3: 157-170.

Dutton, M. G., Hoult N. A., Take W. A. Towards a Digital Image Correlation Based Strain Sensor // The 8th International

Workshop on Structural Health Monitoring. – 2011. – Vol. 4. – P. 2195-2203.

Ni, Q., Hird, C. C., Guymer, I. 2010. Physical modelling of pile penetration in clay using transparent soil and particle image velocimetr.y Geotechnique 60. No. 2. 121-132.

PIVview User Manual. PIVTEC GmbH, Homepage: http://www.pivtec.com (10.10.2011).

Roscoe, K.H., Arthur, J.R.F., James, R.G. 1963. The determination of strain in soils by X-ray method. Civ. Eng. And publ. works Rew. 58. No. 684. 873-876 and No. 685. 1009–1011.

Sevi, A. F., Ge, L., Take, W. A. 2009. A Large-Scale Triaxial Apparatus for Prototype. Railroad Ballast Testing Geotechnical Testing Journal. Vol. 32. 8-16.

White D. J., Take W.A, Bolton M.D., Munachen S.E. 2001. A deformation measuring system for geotechnical testing based on digital imaging, close-range photogrammetry, and PIV image analysis. Proceedings of the 15th International Conference on Soil Mechanics and Geotechnical Engineering. Vol. 1. 539-542.

Zhao H., Ge L. 2008. Camera Calibration Using Neural Network for Image-Based Soil Deformation Measurement Systems // Geotechnical Testing Journal. Vol. 31. No. 2. 192-197.